JACC: BASIC TO TRANSLATIONAL SCIENCE VOL. 3, NO. 5, 2018

PRECLINICAL RESEARCH

Discovery of a Small Molecule to Increase Cardiomyocytes and Protect the Heart After Ischemic Injury

Hironori Hara, MD, PhD,[a] Norifumi Takeda, MD, PhD,[a] Masaki Kondo, BS,[b] Mio Kubota, MSc,[b] Tatsuo Saito, PhD,[b] Junichi Maruyama, PhD,[c] Takayuki Fujiwara, MD, PhD,[a] Sonoko Maemura, MD,[a] Masamichi Ito, MD, PhD,[a] Atsuhiko T. Naito, MD, PhD,[a] Mutsuo Harada, MD, PhD,[a] Haruhiro Toko, MD, PhD,[a] Seitaro Nomura, MD, PhD,[a,d] Hidetoshi Kumagai, PhD,[a] Yuichi Ikeda, MD, PhD,[a] Hiroo Ueno, MD, PhD,[e] Eiki Takimoto, MD, PhD,[a] Hiroshi Akazawa, MD, PhD,[a] Hiroyuki Morita, MD, PhD,[a] Hiroyuki Aburatani, MD, PhD,[d] Yutaka Hata, MD, PhD,[c] Masanobu Uchiyama, PhD,[b,f] Issei Komuro, MD, PhD[a]

VISUAL ABSTRACT

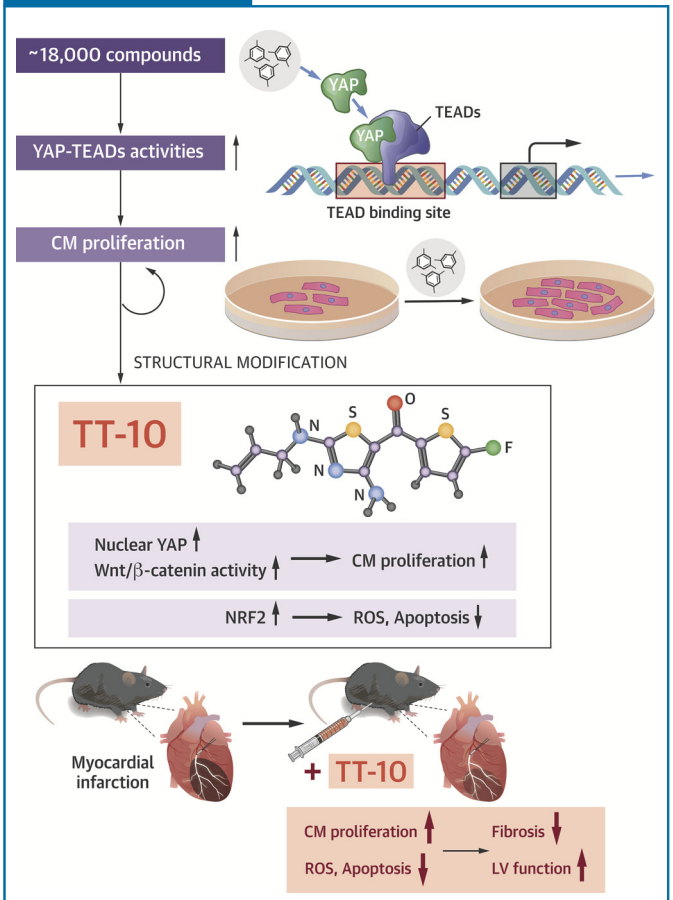

Hara, H. et al. J Am Coll Cardiol Basic Trans Science. 2018;3(5):639–53.

HIGHLIGHTS

- New CMs in adult mammalians are generated at a low rate, and Hippo-YAP signaling plays crucial roles in the postnatal cardiac regeneration.
- After chemical screenings to identify compounds that activate YAP-TEADs activities and CM proliferation in vitro, the authors synthesized a novel multifaceted fluorinated compound TT-10 ($C_{11}H_{10}FN_3OS_2$) from a biologically hit compound.
- TT-10 induces proliferation of cultured CMs via nuclear translocation of YAP and activation of Wnt/β-catenin signaling, and also activates NRF2-mediated antioxidant and antiapoptotic effects.
- The intraperitoneal injection of TT-10 ameliorates cardiac remodeling after MI in mice, which is partially mediated by CM proliferation and by direct antioxidant and antiapoptotic effects in vivo.
- Stimulating CM proliferation and/or protection with TT-10 might complement current therapies for MI.

From the [a]Department of Cardiovascular Medicine, The University of Tokyo Hospital, Tokyo, Japan; [b]Graduate School of Pharmaceutical Sciences, The University of Tokyo, Tokyo, Japan; [c]Department of Medical Biochemistry, Graduate School of Medical and Dental Sciences, Tokyo Medical and Dental University, Tokyo, Japan; [d]Genome Science Division, Research Center for Advanced Science and Technology, University of Tokyo, Tokyo, Japan; [e]Department of Stem Cell Pathology, Kansai Medical

ISSN 2452-302X https://doi.org/10.1016/j.jacbts.2018.07.005

ABBREVIATIONS AND ACRONYMS

BIO = (2′Z,3′E)-6-bromoindirubin-3′-oxime

EdU = 5-ethynyl-2′-deoxyuridine

FGF1 = acidic fibroblast growth factor

MI = myocardial infarction

NRF2 = nuclear factor erythroid 2-related factor 2

NRG1 = neuregulin-1

TAZ = transcriptional coactivator with PDZ-binding motif

TEAD = transcriptional enhancer factor domain

YAP = YES-associated protein

SUMMARY

Accumulating data suggest that new cardiomyocytes in adults are generated from existing cardiomyocytes throughout life. To enhance the endogenous cardiac regeneration, we performed chemical screenings to identify compounds that activate pro-proliferative YES-associated protein and transcriptional enhancer factor domain activities in cardiomyocytes. We synthesized a novel fluorine-containing TT-10 ($C_{11}H_{10}FN_3OS_2$) from the biologically hit compound. TT-10 promoted cardiomyocyte proliferation and simultaneously exerted antioxidant and antiapoptotic effects in vitro. TT-10 treatment in mice ameliorated myocardial infarction–induced cardiac dysfunction at least in part via enhancing clonal expansion of existing cardiomyocytes with nuclear YES-associated protein expression. Stimulating cardiomyocyte proliferation and/or protection with TT-10 might complement current therapies for myocardial infarction. (J Am Coll Cardiol Basic Trans Science 2018;3:639–53)

Cardiomyocytes (CMs) rapidly proliferate during embryonic development and exit the cell cycle soon after birth in mammals; thus, many cell-based therapies for advanced heart failure are currently in progress. However, recent accumulating evidence suggests that new CMs are generated from pre-existing CMs at a low rate throughout life (1,2), decreasing with age and increasing with injury, and the development of pharmacological strategies to stimulate this process may provide a rational alternative treatment or complement current therapies for advanced heart failure.

New CMs are probably derived from existing CMs under normal conditions, but the limited regenerative capacity is unable to restore cardiac function after substantial cardiac damage. Recently, the apex-resected neonatal mouse myocardium has been shown to completely regenerate by retaining and/or enhancing the self-renewal capacity, similar to certain adult vertebrate species, such as teleost fish and urodele amphibians, and this injured myocardium is completely regenerated without fibrosis or scarring after inflammatory responses (3,4). The underlying molecular mechanism for the CM proliferation has been vigorously investigated. Postnatal normobaric oxygen exposure, and the resulting reactive oxygen species (ROS) generation and DNA damage result in CM cell cycle arrest, whereas Wnt/β-catenin signaling and extracellular growth factors, such as neuregulin-1 (NRG1) and acidic fibroblast growth factor (FGF1), could stimulate mature CM cell cycle re-entry and cell division (cytokinesis) (5,6). Thus, many different pharmacological agents have been explored for their potential CM proliferative effects; however, there are no approved therapies for the specific prevention of myocardial infarction (MI)-induced cardiac remodeling.

SEE PAGE 654

Recently, Hippo signaling was also reported to play crucial roles in the regulation of fetal cardiac development and postnatal CM proliferation (7,8). Hippo signaling pathway regulates diverse aspects of cell proliferation, apoptosis, and stemness in response to a wide range of extracellular and intracellular signals. When the Hippo pathway is inactivated, YES-associated protein (YAP) and transcriptional coactivator with PDZ-binding motif (TAZ) accumulate in the nucleus to regulate the DNA-binding activity of transcriptional enhancer factor domain (TEAD), a crucial transcriptional factor that triggers proliferative and prosurvival gene expression programs (9). CM-specific *Yap*-knockout

University, Osaka, Japan; and the [f]Advanced Elements Chemistry Research Team, RIKEN Center for Sustainable Resource Science, and Elements Chemistry Laboratory, RIKEN, Saitama, Japan. This study was supported by grants-in-aid for scientific research (to Drs. Hara, Takeda, Saito, Uchiyama, and Komuro); grants-in-aid from Japan Foundation for Applied Enzymology (to Drs. Hara and Takeda); grants-in-aid from the Kanae Foundation for the Promotion of Medical Science, SENSHIN Medical Research Foundation, Japan Heart Foundation, The Tokyo Society of Medical Sciences, Takeda Science Foundation, and The Fugaku Trust for Medical Research (to Dr. Takeda); and grants-in-aid from the Daiichi-Sankyo Award in Synthetic Organic Chemistry, Japan (to Dr. Saito). All other authors have reported that they have no relationships relevant to the contents of this paper to disclose.
All authors attest they are in compliance with human studies committees and animal welfare regulations of the authors' institutions and Food and Drug Administration guidelines, including patient consent where appropriate. For more information, visit the *JACC: Basic to Translational Science* author instructions page.

Manuscript received March 29, 2018; revised manuscript received May 22, 2018, accepted July 17, 2018.

mice (*αMHC-Cre*; $Yap^{floxed/floxed}$) impair the regenerative capacity of the neonatal heart, and transgenic mice with CM-specific expression of constitutively activated form of YAP (YAP-S112A) retain cardiac regenerative activity after cardiac MI even in adults (8). In addition, the Hippo pathway has been recently reported to cross-talk with Wnt/β-catenin signaling, which may also play prominent roles in modulations of CM proliferation activity and cardiac lineage/fate decisions (10).

Here, based on these observations, we executed 2 different cell-based large-scale chemical screenings to identify chemical compounds that could increase YAP-TEAD activity and protect the heart against ischemic injury. A fluorine substituent (TT-10) derived from the biologically active compound (TAZ-12) strongly promoted CM proliferation and showed antioxidant and antiapoptotic effects in vitro. The intraperitoneal injection of TT-10 in mice subjected to MI promoted CM cell-cycle activities and protection, which resulted in amelioration of cardiac dysfunction. Thus, TT-10, a novel and multifaceted compound, may provide a treatment strategy that complements current therapies for patients with MI.

METHODS

A detailed description of Methods is found in the Supplemental Appendix.

CELL-BASED SCREENING ASSAYS FOR YAP-TEADs ACTIVATORS. The library of approximately 18,600 chemicals that were screened was provided by the Chemical Biology Screening Center at Tokyo Medical and Dental University.

1. For fluorescence reporter-based assay for YAP-TEAD activators, ARPE-19 cells were transfected with the pLL3.7-K122 FH-YAP1-ires-GFP-TEADs-responsive-promoter-H2B-mCherry reporter using Lipofectamine 2000 (Thermo Fisher Scientific, Waltham, Massachusetts). The YAP1-expressing ARPE-19 cells were treated with 10 μmol/l of each compound for 72 h, and the H2B-mCherry signal inside the nucleus was measured (11).
2. For sphere formation assay for TAZ activators, human breast epithelial MCF10A cells expressing TAZ (MCF10A-TAZ) were cultured with 10 μmol/l of each compound for 10 days, and TAZ activators enabled TAZ-expressing MCF10A cells to form spheres (12). The TEAD reporter assay for 50 putative TAZ activators was performed with HEK293 cells.

CM PROLIFERATION ASSAY. To detect DNA synthesis in proliferating CMs, CMs were incubated with 5 μmol/l 5-ethynyl-2'-deoxyuridine (EdU) under starved conditions (0.1% fetal calf serum [FCS]). After 40 h, incorporated EdU in CMs was stained with the Click-iT EdU detection reagent (Thermo Fisher Scientific). To detect nuclear division (karyokinesis) and cell division (cytokinesis), cells were stained with antibodies against phosphohistone H3 (pH3) (Millipore, Burlington, Massachusetts) and aurora B kinase (Cell Signaling, Danvers, Massachusetts), respectively.

ANIMALS. *αMHC-MerCreMer* (13) and $Rosa26^{rbw/+}$ (14) mice have been previously described. C57BL/6J mice were purchased from CLEA Japan, Inc. (Tokyo, Japan). All experiments were approved by the University of Tokyo Ethics Committee for Animal Experiments and strictly adhered to the guidelines of the University of Tokyo for animal experiments. All personnel involved in data collection and analysis were blinded to treatment allocation.

MI MODEL. MI was performed as previously described (15). MI mice were randomly assigned in a 1:1 ratio to receive vehicle or TT-10 after the MI procedure, according to each experimental protocol as described in detail elsewhere.

LINEAGE TRACING OF EXISTING CMs. Lineage tracing experiments of existing CMs were performed to evaluate clonal proliferation. *αMHC-MerCreMer;* $Rosa26^{rbw/+}$ mice were injected intraperitoneally with a single low dose of tamoxifen (5 mg/kg body weight [Sigma-Aldrich, St. Louis, Missouri]). After Cre-mediated recombination, 1 of the 3 fluorescent marker proteins (mOrange, mCerulean, or mCherry) was stochastically placed under the control of CAG promoter. mOrange was the brightest and most easily detected; thus, we selected mOrange-expressing CMs for subsequent analysis. Approximately 3% of existing CMs irreversibly expressed mOrange after tamoxifen treatment, and approximately 2% of mOrange-labeled CMs in MI (−) mice formed a cluster 1 week after sham operation, which presumably consisted of both simply adjacent CMs and spontaneously divided CMs. The increase in the proportion of clustered labeled CMs was considered to be attributed to the additional proliferation of existing CMs (clonal expansion) after MI and TT-10 treatment, and evaluated. Horizontal sections of the ventricles were freshly embedded in OCT compound, sectioned at a thickness of 10 μm, and collected at 700-μm intervals. Digital images of 5 different sections were captured and evaluated. Detailed methods are described in the Supplemental Material.

FIGURE 1 **Generation of the Novel Fluorinated Compound TT-10**

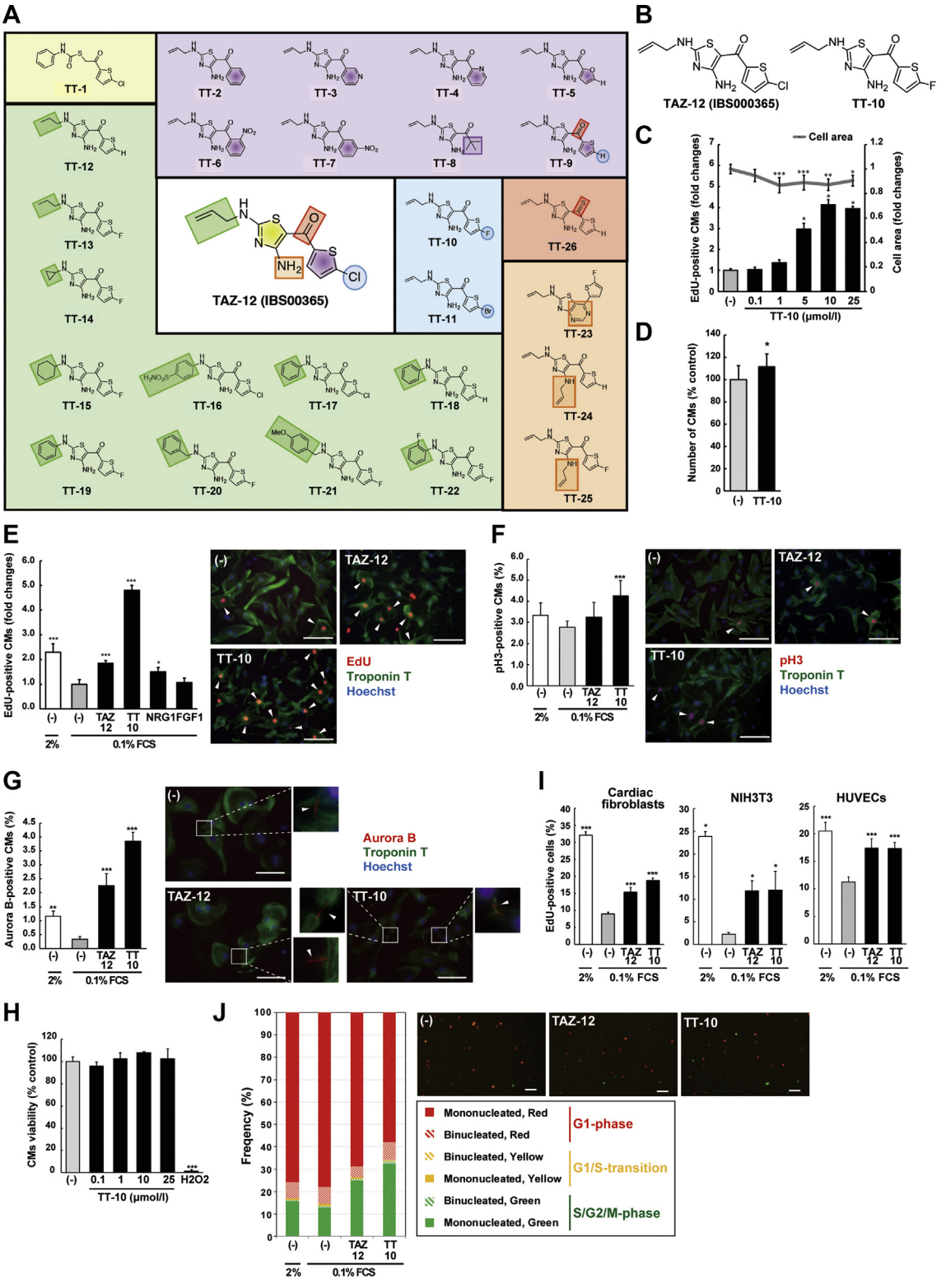

Continued on the next page

MEASUREMENT OF MYOCARDIAL INFARCT SIZE AND FIBROSIS. Horizontal sections of the ventricles were collected at 700-μm intervals. Sections were stained with Picrosirius Red/Fast Green dyes. Digital images of 5 different sections were captured and evaluated. Infarct size was calculated as a percentage of entire left ventricular (LV) volume (16). The percentage of LV fibrotic area was assessed by areas of red and green-stained regions using ImageJ software (National Institutes of Health, Bethesda, Maryland).

STATISTICS. All analyses were performed using JMP Pro 13.0.0 (SAS Institute Inc., Cary, North Carolina). Data are shown as mean ± SD. The assumption of homogeneity of variance was tested using Levene's test. The significance of differences among means was evaluated using a Student's *t*-test, Welch's t-test, 1-way analysis of variance followed by post hoc Tukey-Kramer test, or Kruskal-Wallis test followed by post hoc Steel-Dwass test. All p values <0.05 were considered statistically significant.

RESULTS

CELL-BASED ASSAYS FOR YAP-TEADs ACTIVATORS. To identify chemical compounds that enhance the transcriptional activities of TEADs, we performed 2 different cell-based large-scale screenings. In the first assay, mCherry-fused histone 2B protein was expressed under the TEAD-responsive promoter in YAP-expressing ARPE-19 epithelial cells and exposed to each of the 18,606 test compounds (10 μmol/l) (Supplemental Figure 1A). Intranuclear mCherry signal intensity was measured to assess YAP-TEAD complex-dependent transcriptional activity. Based on this measurement, we selected 47 putative YAP-TEAD activators (YAP-1 to -47) (Supplemental Figure 1A) (11). Another screening for TEAD activators was performed using 50 putative activators of the transcriptional coactivator TAZ. These compounds were previously identified from 18,458 chemical compounds using a TAZ activation-dependent sphere-forming assay with MCF10A-TAZ epithelial cells (Supplemental Figure 1B) (12). We performed the TEADs luciferase reporter assay with YAP-expressing HEK293 cells exposed to each of the 50 putative compounds (10 μmol/l). A total of 17 compounds (TAZ-1 to -17) were identified as positive, and all of these compounds were distinct from YAP-1 to -47. Thus, we identified 2 nonoverlapping sets of putative YAP-TEAD activators (YAP-1 to -47 and TAZ-1 to -17) that likely reflect, at least in part, differences between cell types and different levels of test sensitivity and specificity used in the screening processes.

SCREENING FOR CHEMICAL AS ENHANCING CM PROLIFERATION. To evaluate the CM proliferative efficacy of the 64 compounds, we performed an automated fluorescence microscopy-based cell screening using neonatal rat CMs (Supplemental Figure 2A). Cultured CMs treated with each compound (10 μmol/l) were exposed to EdU, a uridine analogue that is incorporated into forming strands of DNA, under starved conditions (0.1% FCS). After incubation, DNA synthesis in the cardiac troponin T-stained CMs was evaluated. The majority of compounds decreased DNA synthesis, but 3 compounds (TAZ-12, YAP-22, and YAP-26) showed more potent DNA forming activity when compared with untreated control subjects (Supplemental Figures 2B and 2C). DNA synthesis occurs in polyploid and/or multinucleated CMs; thus, we evaluated the effects of TAZ-12, YAP-22, and YAP-26 on CM karyokinesis and cytokinesis using cell staining against pH3 and aurora B kinase, respectively. TAZ-12 (IBS000365; $C_{11}H_{10}ClN_3OS_2$) (**Figures 1A and 1B**) significantly enhanced both staining (Supplemental Figures 3A and 3B).

STRUCTURE-ACTIVITY RELATIONSHIPS. To improve the CM proliferative activity, we next examined the structure-activity relationships chemically focused

FIGURE 1 Continued

(A) Chemical structures of the 26 analogues of TAZ-12. The chemical structure modified is highlighted with a **colored circle or square**. **(B)** Chemical structures of TAZ-12 and TT-10. **(C)** Ratios of 5-ethynyl-2′-deoxyuridine (EdU)–positive cardiomyocytes (CMs) and mean CM size 40 h after treatment with the indicated concentrations of TT-10. n = 7 per group. **(D)** Relative cell number of CMs 40 h after treatment with TT-10 (10 μmol/l), relative to untreated CMs. n = 12 per group. **(E)** Ratios of EdU-positive CMs after the treatment with indicated reagents at the following concentrations: TAZ-12, 10 μmol/l; TT-10, 10 μmol/l; NRG1, 100 ng/ml; and acidic fibroblast growth factor (FGF1), 100 ng/ml. Representative images of TAZ-12– and TT-10–treated CMs are shown. The relative values are normalized to the untreated control. **Arrowheads** indicate positive CMs. n = 4 per group. Scale bar: 100 μm. **(F and G)** Percentages of pH3-positive **(F)** and Aurora B-positive **(G)** CMs after treatment with TAZ-12 and TT-10. Representative images are shown. **Arrowheads** indicate positive CMs. n = 8 **(F)** and n = 4 **(G)** per group. Scale bar: 100 μm in **A**; 50 μm in **B**. **(H)** MTS cell viability assay. The positive control was 100 μmol/lH_2O_2. n = 3 per group. **(I)** Effects of TAZ-12 and TT-10 on proliferative activities of non-CMs. Rat cardiac fibroblasts, NIH3T3 fibroblasts, and human umbilical vein endothelial cells (HUVECs) were cultured for 24, 18 and 18 h, respectively. n = 5 (rat cardiac fibroblasts), n = 7 (NIH3T3 fibroblasts), and n = 5 (HUVECs) per group. **(J)** Percentages of mono- or binucleated CMs. Representative images are shown. CMs infected with Fucci-expressing adenoviruses under the *Tnnt2* promoter were treated with TAZ-12 (10 μmol/l) and TT-10 (10 μmol/l) for 40 h. n = 4 per group. Scale bar: 100 μm. *p < 0.05, **p < 0.01, and ***p < 0.001 versus the untreated control.

on each colored square position of TAZ-12 (Figure 1A). Initially, we investigated ring-opening structure (TT-1) (shown in the yellow square position of Figure 1A), but this resulted in significant loss of DNA-forming activity (Supplemental Figure 4A). These results imply that the *N*-allyl thiazole unit is involved in the DNA synthesis of CMs. Then, retaining *N*-allyl thiazole moiety, we probed the thiophene unit in the purple square position. Replacement of 5-chlorothiophene with another aromatic ring (TT-2, -3, -4, -5, -6, or -7) or *tert*-butyl group (TT-8) decreased DNA forming activity, whereas TT-9 (thiophene) maintained the CM proliferation (Supplemental Figure 4A). As for the halogen at the 5-position of thiophene ring in the aqua circle position, 5-fluorothiophene (TT-10) showed the best result, and 3-fold enhanced DNA forming activity even compared with the 2% FCS-containing pro-proliferative condition (Supplemental Figure 4B). We examined the *N*-alkyl chain at the 2-position of thiazole further in depth (shown in green square position of Figure 1A). The linear-alkyl chain (TT-12 or -13) maintained DNA synthesis activity, whereas cyclic alkane (TT-14 or -15) and aromatic substituents (TT-16, -17, -18, -19, -20, -21, or -22) induced CM death (Supplemental Figure 4A) (cytotoxic activity not shown). Interestingly, cyclohexane analogue (TT-15) was the most effective for DNA synthesis of CMs only under high-dilution conditions (1 μmol/l; data not shown). We assume the substituent in the green square is deeply related to cytotoxicity. TT-10 can form either conformer I (linear structure) or II (bent structure using the intramolecular hydrogen bond between the carbonyl and amino group) (shown in Supplemental Figure 4C). To understand the influence of these conformers and the role of primary amine at the 4-position of the thiazole ring on CM proliferation, we designed and prepared TT-23 (fixed in conformation II by pyrimidine ring) and *N*-allyl modifications (TT-24 and -25), respectively. However, all of them displayed poor activity (Supplemental Figure 4A), and thus a linear structure seems necessary for the CM proliferative activity. Moreover, a thiocarbonyl derivative (TT-26) showed no improvement (in the red square position) (Supplemental Figure 4A). Fluorine-containing molecules, such as TT-10, have recently gained considerable attention because of the metabolic stability of the carbon-fluorine bond against enzymatic degradation, which effectively increases the in vivo bioavailability (17). Taking these results together, we selected TT-10 ($C_{11}H_{10}FN_3OS_2$) for further examination (Figure 1B).

EFFECTS OF TT-10 ON RAT NEONATAL CM PROLIFERATION. TT-10 induced DNA synthesis in a concentration-dependent manner, and the treated CMs became smaller in size (Figure 1C). TT-10 increased the absolute number of cultured CMs (Figure 1D), and DNA synthesis activity at a 10 μmol/l concentration was more prominent than the well-known proliferative activities of NRG1 and FGF1 (Figure 1E). In addition, TT-10 significantly enhanced both CM pH3-positive karyokinesis and aurora B-positive cytokinesis (Figures 1F and 1G), and TT-10 did not show toxicity against cultured CMs (Figure 1H). On the other hand, the TT-10-mediated effect on proliferation of non-CMs, including rat neonatal cardiac fibroblasts, NIH3T3 fibroblasts, and human umbilical vein endothelial cells, was much smaller when compared with cells treated with 2% FCS (Figure 1I), whereas the activity in CMs was much stronger than 2% FCS (Figure 1E). To confirm this CM cell cycle promoting activity, we developed a new automated evaluation system that used adenoviruses for the CM-specific expression of fluorescent, ubiquitination-based cell cycle indicators (18). Rat cardiac troponin T (*tnnt2*) promoter-driven fluorescent, ubiquitination-based cell cycle indicators label G1-phase CMs with red fluorescence (Kusabira-Orange2; mKO2) and S/G2/M-phase CMs with green fluorescence (Azami-Green1; mAG1) (Supplemental Figures 5A to 5D) and distinguish between mononucleated and binucleated CMs (Supplemental Figure 5E). When exposed to TT-10, the number of CMs in the S/G2/M-phase was significantly increased, but the proportions of mono- and binucleated CMs were similar to CMs under starved culture conditions (Figure 1J). Taken together, TT-10 induces quiescent cultured CMs to re-enter the cell cycle and undergo karyokinesis and cytokinesis in vitro; furthermore, this proliferative effect was relatively strong for CMs.

TT-10 AFFECTS TEADs ACTIVITIES IN CMs. To examine the mechanism of increased CM proliferation, we first assessed whether TT-10 enhanced TEAD activities in CMs in a similar manner as that of epithelial cells. TEAD-dependent luciferase activity was increased in CMs treated with TT-10 (10 μmol/l) (Figure 2A) without increasing YAP or TAZ expression (Supplemental Figure 6A). We next examined the influence on subcellular localization of YAP and TAZ. They were located predominantly in the CM nuclei even at nearly confluent conditions; however, TT-10 further enhanced the nuclear expression of YAP, but not TAZ (Figure 2B, Supplemental Figure 6B), indicating that TT-10 enhances CM proliferation, at least in part, via nuclear translocation of YAP.

FIGURE 2 TT-10 Activates YAP-TEADs Activity and the Wnt/β-Catenin Signaling Pathway

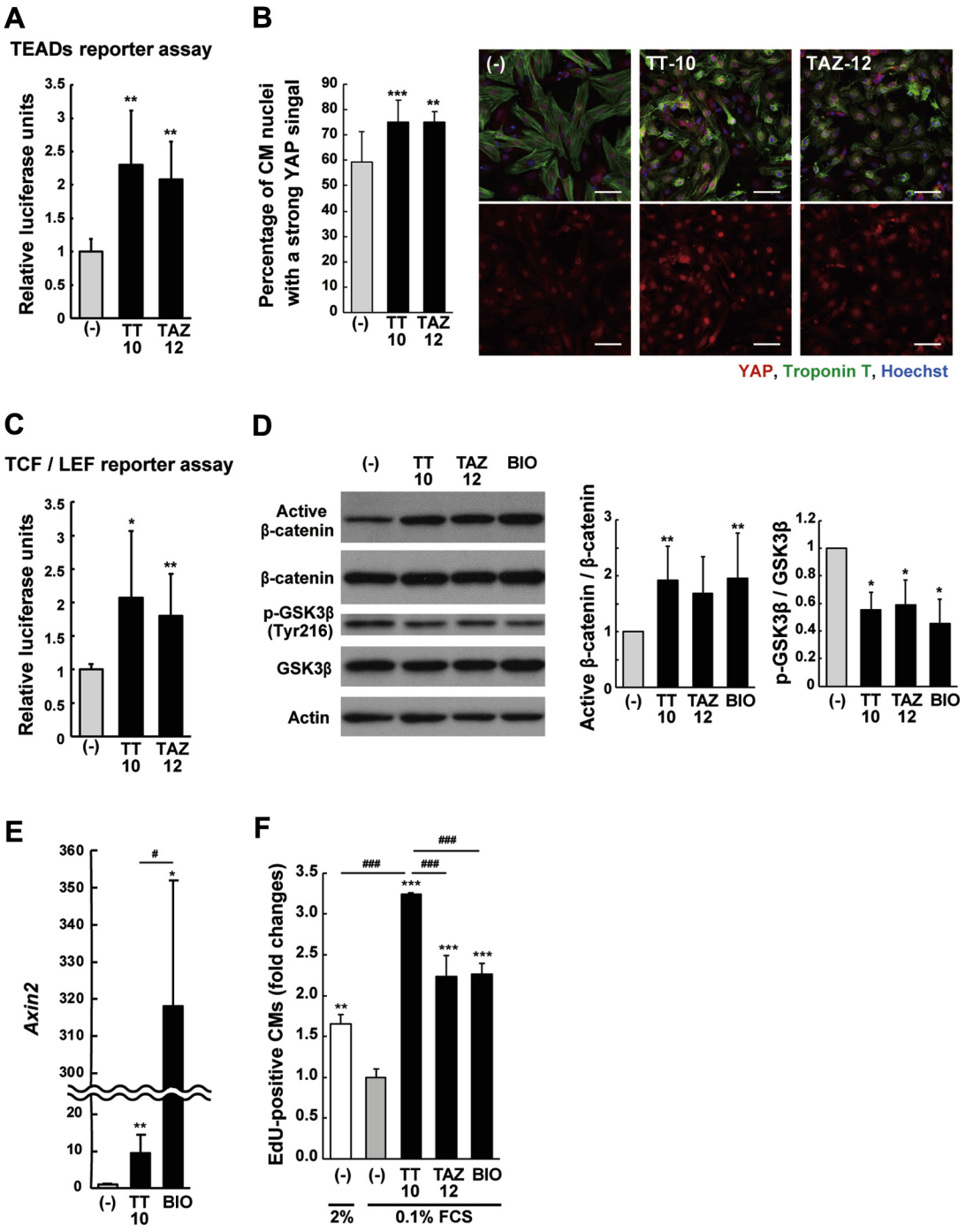

(A) Transcriptional enhancer factor domain (TEAD) reporter activity in CMs treated with TT-10 and TAZ-12. n = 9 per group. **(B)** Quantitative imaging assay for YES-associated protein (YAP) nuclear translocation. CMs were treated with TT-10 and TAZ-12 (10 μmol/l). n = 12 (untreated control and TT-10) and 9 (TAZ-12). Scale bar: 50 μm. **(C)** TCF/LEF reporter activity in CMs treated with TT-10 and TAZ-12. n = 7 per group. **(D)** Western blot analysis of Wnt/β-catenin signaling pathway-related proteins. CMs were treated with the indicated reagents at the following concentrations for 6 h: TT-10, 10 μmol/l; TAZ-12, 10 μmol/l; (2′Z,3′E)-6-bromoindirubin-3′-oxime (BIO), 1 μmol/l. n = 6 to 7 per group. **(E)** Relative expression of *Axin2* in CMs treated with TT-10 and BIO for 24 h. n = 7 (untreated), 7 (TT-10), and 4 (BIO). **(F)** Ratios of EdU-positive CMs 40 h after the treatment with TT-10, TAZ-12, and BIO. n = 3 per group. *p < 0.05, **p < 0.01, and ***p < 0.001 versus the untreated control. #p < 0.05 and ###p < 0.001 versus TT-10. Abbreviations as in Figure 1.

FIGURE 3 Transcriptome Analysis of CMs Treated With TT-10

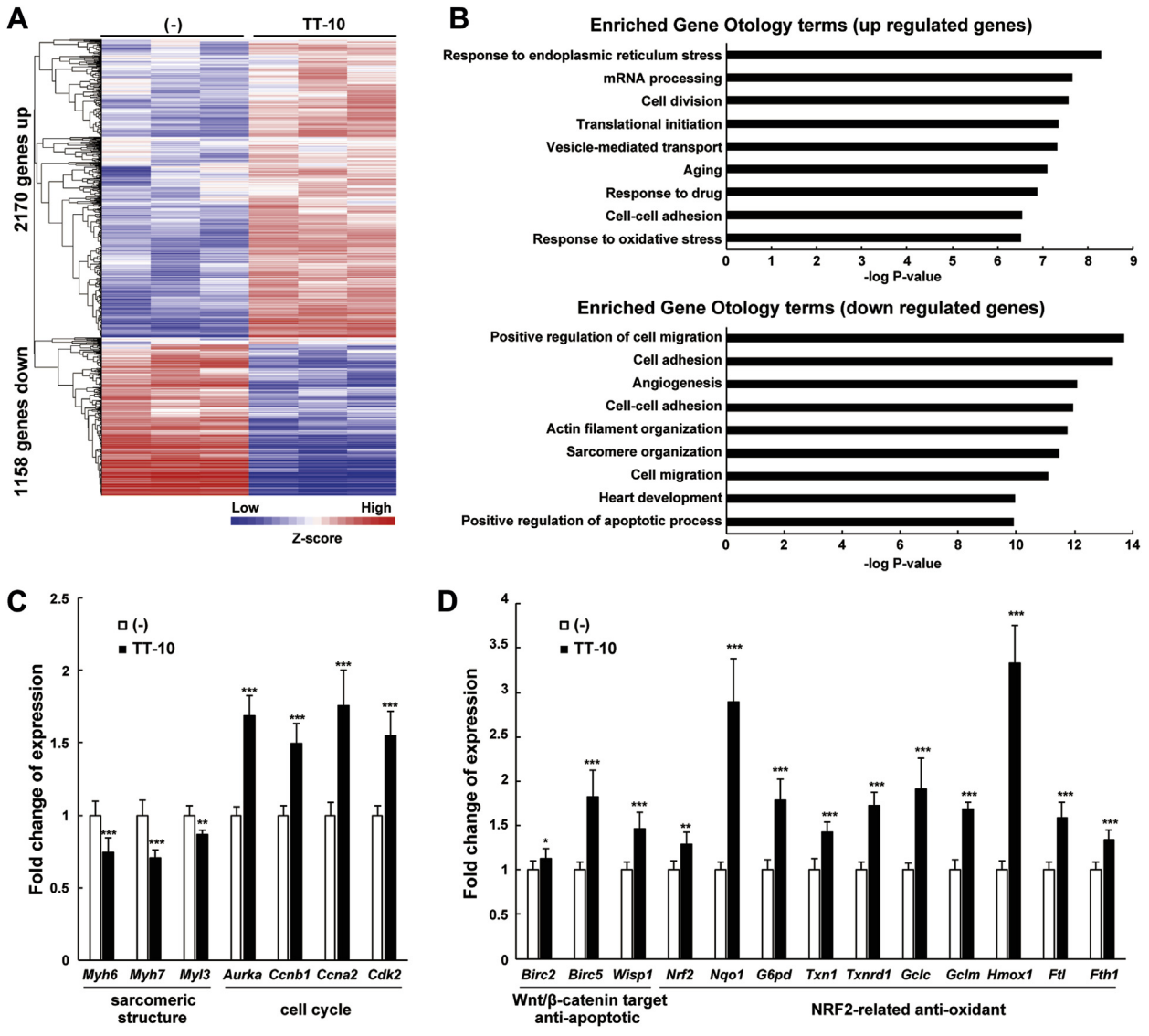

(A) Transcriptome analysis of CMs treated with TT-10. Heatmap comparison represents gene expression changes. Starved CMs were treated with vehicle or 10 μmol/l TT-10 for 24 h and harvested for RNA-Seq transcriptomic profiling. **(B)** GO term enrichment analysis of up- and down-regulated genes. **(C and D)** Relative expression of selected genes involved in the formation of sarcomeric structures and cell cycle regulation **(C)** and Wnt/β-catenin and NRF-2 signaling **(D)** were measured using quantitative real-time polymerase chain reaction. n = 7 per group. *p < 0.05, **p < 0.01, and ***p < 0.001 versus the untreated control group. Abbreviations as in Figure 1.

TT-10 ACTIVATES THE WNT/β-CATENIN SIGNALING PATHWAY. We examined the activation of the Wnt/β-catenin signaling pathway, which may interact with the Hippo pathway (7) and participate in the regulation of CM proliferation (19). CMs transfected with a Wnt/β-catenin-responsive element luciferase reporter (TCF/LEF-Luc) and treated with TT-10 (10 μmol/l) showed a significant increase in the reporter activity (Figure 2C), which was supported by increased nonphospho (active) β-catenin, and Wnt/β-catenin target gene *Axin2* expression (Figures 2D and 2E). The phosphorylation and degradation of β-catenin are promoted by active (phosphorylated) GSK3β (20). TT-10 inhibited GSK3β phosphorylation at Tyr-216 residue (Figure 2D, Supplemental Figure 7A), which may have caused the subsequent activation of

FIGURE 4 Antioxidant and Antiapoptotic Activities of TT-10 in CMs

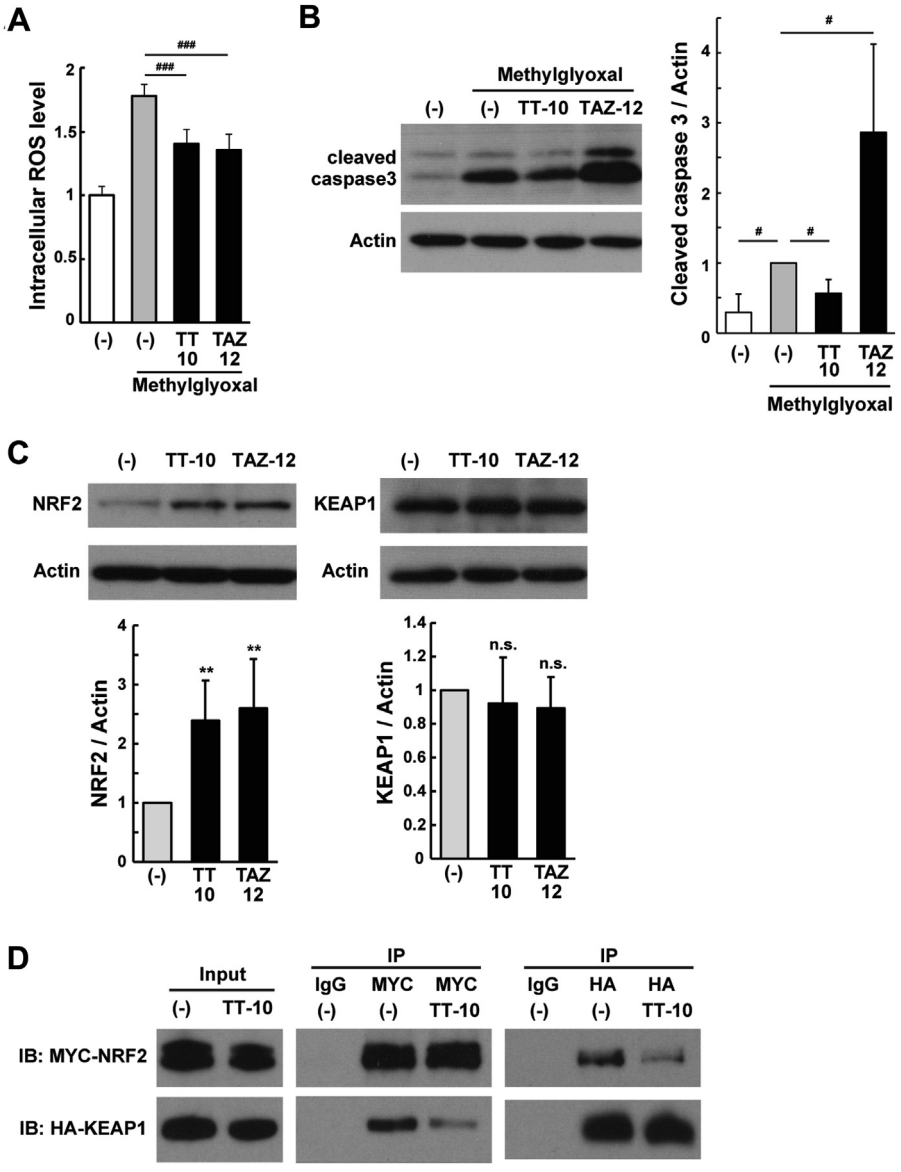

(A) Intracellular reactive oxygen species (ROS) production was induced by methylglyoxal (100 μmol/l). n = 4 per group. **(B)** Western blot analysis of cleaved caspase 3. Starved CMs were treated with 10 μmol/l of each compound for 18 h. Next, 1 mmol/l methylglyoxal was added, and CMs were cultured for 6 h. n = 5 per group. **(C)** Western blot analysis of NRF2 and KEAP1. CMs were treated with 10 μmol/l of each compound for 6 h. n = 7. **(D)** Coimmunoprecipitation assay. The MYC3-NRF2 and HA2-KEAP1–overexpressing HEK293 cells were treated with TT-10 (10 μmol/l) for 2 h. Cell lysates were immunoprecipitated with mouse immunoglobulin G, anti-MYC-tag, or anti-HA-tag antibody. Cell lysates (input), IgG immunoprecipitates (IP), anti-MYC IP, and anti-HA IP were probed with anti-MYC-tag and anti-HA-tag antibodies. n.s. $p > 0.05$, **$p < 0.01$ versus the untreated control. #$p < 0.05$, ###$p < 0.001$ versus the methylglyoxal-treated control. Abbreviations as in Figure 1.

Wnt/β-catenin signaling. TT-10 was more effective at promoting DNA synthesis when compared with the GSK3β inhibitor BIO ([2′Z,3′E]-6-bromoindirubin-3′-oxime) (1 μmol/l, a suitable dose for CM proliferation without toxicity; data not shown) (Figure 2F) (21), even though GSK3β phosphorylation was inhibited to the same extent and the TT-10-mediated induction of *Axin2* was much less than BIO (Figures 2D and 2E). BIO

FIGURE 5 TT-10 Ameliorates Cardiac Dysfunction After MI in Mice

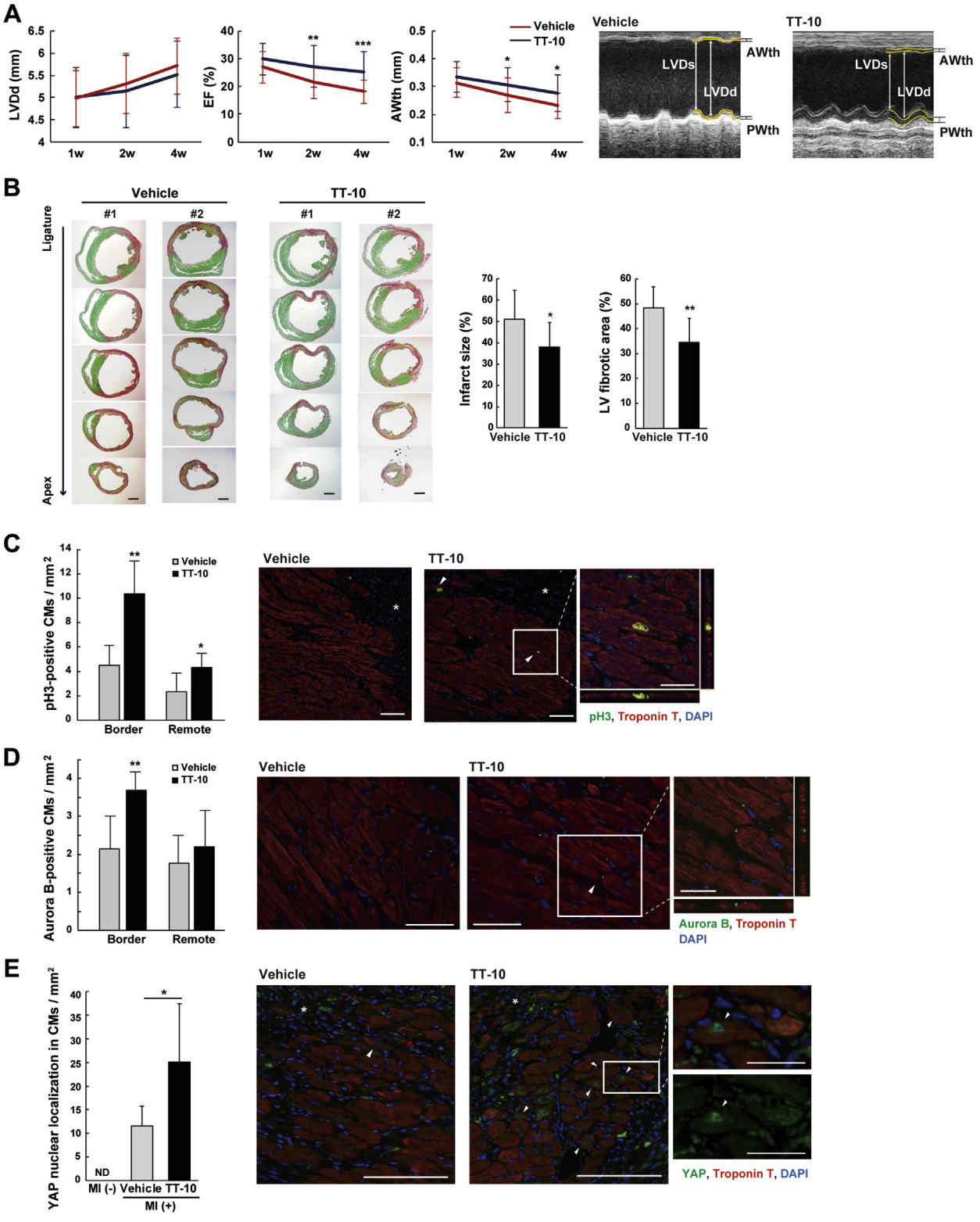

Continued on the next page

did not enhance nuclear expression of YAP (Supplemental Figure 7B), and other CM proliferative signals, such as phosphorylation of extracellular signal regulated kinase and AKT induced by NRG1 and FGF1, were not activated by TT-10 (Supplemental Figure 7C). Thus, the promotion of CM proliferation by TT-10 might be explained by activation of the Wnt/β-catenin signaling, in addition to the effect on YAP nuclear translocation.

TT-10 HAS ANTIOXIDANT AND ANTIAPOPTOTIC ACTIVITIES IN CMs. To further elucidate the effects of TT-10, next-generation sequencing-based transcriptome analysis (RNA-seq) was performed on cultured CMs treated with vehicle or TT-10 (**Figure 3A**). Gene ontology (GO) term enrichment analysis of the 3,328 identified genes revealed that cell division genes were up-regulated and genes associated with sarcomere and actin cytoskeleton organization were down-regulated (**Figure 3B**). This finding is consistent with dedifferentiation and sarcomere disassembly in CMs re-entering the cell cycle (3). Quantitative real-time polymerase chain reaction of selected genes confirmed that sarcomere-associated genes were down-regulated and genes involved in the cell cycle were up-regulated (**Figure 3C**). In addition, the GO analysis revealed that TT-10 may have antioxidant and antiapoptotic functions, which would be beneficial for the survival of damaged CMs (**Figure 3B**). Quantitative real-time polymerase chain reaction analysis revealed the up-regulation of target genes of Wnt/β-catenin with antiapoptotic activities, and target genes of NRF2 (nuclear factor erythroid 2-related factor 2: a master regulator of antioxidant transcriptional responses) (**Figure 3D**). TT-10 inhibited methylglyoxal (a precursor of advanced glycation end-products)-induced ROS production and activation (cleavage) of caspase-3 protein, a marker for apoptosis, whereas TAZ-12 enhanced apoptosis (**Figures 4A and 4B**). Accordingly, TT-10 enhanced TAZ-12-mediated CM proliferation and favorably decreased the pro-apoptotic action of TAZ-12.

To further examine this antioxidant mechanism, we focused on the NRF2-mediated antioxidant system. The transcription factor NRF2 is degradated by the KEAP1-mediated ubiquitin-proteasome system; however, oxidative stress causes NRF2 to dissociate from NRF2-KEAP1 complex and subsequently translocate into the nucleus to positively regulate antioxidant genes (22). When CMs were treated with TT-10, NRF2 expression was significantly increased, whereas KEAP1 expression was unchanged (**Figure 4C**, Supplemental Figure 8A). In addition, TT-10 promoted the dissociation of NRF2-KEAP1 complex in HEK293 cells cotransfected with MYC3-NRF2 and HA2-KEAP1 (**Figure 4D**). These results suggest that the antioxidant effects of TT-10 are mediated, at least in part, by increasing expression levels and nuclear translocation of NRF2. However, NRF2 activation by sulforaphane (a phytochemical in broccoli sprouts) reduced DNA synthesis and siRNA-mediated NRF2 knockdown had no effect on DNA synthesis (Supplemental Figures 8B and 8C), suggesting that NRF2 alone has no positive effect on CM proliferation.

TT-10 IMPROVES CARDIAC FUNCTION AFTER MI. We examined the in vivo effects of TT-10 on cardiac repair after experimental MI in mice, which was induced by surgical permanent ligation of the left anterior descending coronary artery (Supplemental Figure 9A). Intraperitoneal injection of TT-10 (10 mg/kg body weight) did not affect general behavior, appearance, survival, weights of body and organs, blood tests of liver and kidney functions, or cardiac function in sham-operated mice (Supplemental Figure 9B, data not shown). In contrast, TT-10 administration increased echocardiographic LV wall thickness and significantly improved systolic function in mice subjected to MI (**Figure 5A**). Histological studies 1 week after MI revealed that the infarct size and Picrosirius Red–stained fibrotic area were significantly attenuated in TT-10–treated MI mice (**Figure 5B**), and concomitantly, MI-induced CM hypertrophy and decreased CM nuclear density were also ameliorated (Supplemental Figure 10).

FIGURE 5 Continued

(A) Echocardiographic analysis after myocardial infarction (MI). Representative images are shown. n = 23 to 24 (vehicle) and n = 22 to 23 (TT-10). **(B)** Fractional areas of infarction and fibrosis as determined by Picrosirius Red/Fast Green staining and representative cross sections of the hearts from 2 mice (#1 to 2) per group. n = 8 (vehicle) and n = 11 (TT-10). Scale bar: 1 mm. **(C and D)** Quantitative analyses of pH3-positive CMs **(C)** and Aurora B-positive CMs **(D)** 1 week after MI. Representative images of the infarct border-zone myocardium are shown. Inset images were enlarged by z-stack confocal microscopy. **Arrowheads** indicate positive CMs. **White asterisks** indicate infarct area. n = 6 per group. Scale bars in **C and D**: 50 μm (25 μm in insets). **(E)** Nuclear YAP expression in infarct border-zone CMs with representative images. Nuclear YAP expression was not detected in sham operated mice heart. CMs restored YAP activation after MI, and TT-10 treatment further enhanced the numbers of such CMs. ND = not detected. **White asterisks** indicate infarct area. n = 3 (MI [−]), 4 (vehicle), and 6 (TT-10). Scale bars: 100 μm (25 μm in inset). *p < 0.05, **p < 0.01, ***p < 0.001 versus vehicle control. AWth = anterior wall thickness; EF = ejection fraction; LVDd = left ventricular end-diastolic dimensions; LVDs = left ventricular end-systolic dimension; PWth = posterior wall thickness; other abbreviations as in **Figures 1 and 2**.

TT-10 ENHANCES PROLIFERATION OF EXISTING CMs AFTER MI. We next examined the contribution of TT-10-mediated CM proliferation to in vivo cardiac repair after MI. One week after the MI procedure, TT-10 treatment significantly increased the number of pH3- and aurora B-positive CMs at the ischemic border zone (**Figures 5C and 5D**). In addition, TT-10 treatment significantly enhanced the number of CMs with nuclear YAP expression, which was activated in the border zone after MI (**Figure 5E**). To further analyze the clonal expansion of existing CMs during cardiac repair, we traced the lineage of existing CMs in adult *αMHC-MerCreMer*; *Rosa26*$^{rbw/+}$ mice (13,14). After a single exposure to low-dose tamoxifen (5 mg/kg body weight), approximately 3% of existing CMs irreversibly expressed mOrange, and an increase in the number of clustered mOrange-labeled CMs when compared with the control indicates the proliferation of existing CMs. The MI procedure increased the proportion of clustered-labeled CMs by 2.7% at the border zone, and TT-10 treatment further promoted the proliferation of existing CMs (**Figure 6A,** Supplemental Figure 11). Taken together, TT-10 treatment ameliorates cardiac remodeling after MI, which is mediated, at least in part, by the enhanced proliferation of existing CMs.

TT-10 REDUCES ROS PRODUCTION, DNA DAMAGE AND APOPTOSIS AFTER MI. Finally, we examined the antioxidant effect of TT-10 on in vivo cardiac repair after MI, because the increased ROS production in the heart after injury reduces CM proliferative activity (5) and suppression of ROS production reduces cardiac fibrosis (23). In vivo ROS assay using a nuclear localized ROS-sensitive CellROX fluorescent probe revealed that MI induced ROS production at the border zone 1 week after MI procedure, which was reduced by TT-10 treatment (**Figure 6B**). At the same time, TT-10 treatment significantly reduced the number of CMs with phosphorylated H2AX (γH2AX), a sensitive marker of DNA double-strand breaks, and terminal deoxynucleotidyl transferase-mediated dUTP nick-end labeling-positive apoptotic CMs at the infarct border zone 1 week after the MI procedure (**Figure 6C**, Supplemental Figure 12). Decreased ROS production, and simultaneous inhibitory effects on DNA damage and apoptosis by TT-10 treatment might also contribute to the preferable effects on cardiac fibrosis and CM proliferation after MI.

DISCUSSION

In this report, we demonstrate that a novel multifaceted fluorinated compound, TT-10, can induce proliferation of cultured CMs by enhancing YAP-TEAD activities and Wnt/β-catenin signaling, and that TT-10 can protect cultured CMs from oxidative stress and resultant apoptosis by activating NRF2 transcription factor. The intraperitoneal injection of TT-10 ameliorates cardiac remodeling after MI in mice, which is partially mediated by CM proliferation and by direct antioxidant and antiapoptotic effects in vivo (Supplemental Figure 13).

Accumulating evidence suggests that new CMs are generated from existing CMs at a low rate throughout life (1,2), and thus, enhancement of the endogenous CM proliferation for the purpose of compensation for CM death may be a promising strategy for MI (24). Recently, the Hippo-YAP/TAZ-TEADs pathway has been shown to exert powerful growth regulatory activity in CMs; thus, we conducted cell-based large-scale chemical screenings to identify small-molecule activators of TEADs in this study. We have screened over 18,000 compounds based on TEAD transcriptional activities, and 1 fluorine substituent (compound TT-10), derived from a biologically active compound (TAZ-12), was successfully developed to enhance CM proliferation in vitro and in vivo.

The precise mechanisms and specific molecular target underlying the CM proliferative activity of TT-10 should be further analyzed, but activation of Wnt/β-catenin signaling may also be involved, in addition to the enhancement of YAP-TEAD activities. The role of the Wnt/β-catenin signaling in CM proliferation has been controversial. Activation of β-catenin in the heart by adenovirus-mediated expression of constitutively active β-catenin (19), and treatment with GSK3β inhibitor (BIO) attenuate LV remodeling after MI injury in rodents (25). In contrast, administration of a homologous peptide fragment of Wnt3a/Wnt5a (UM206), which serves as a Wnt antagonist and reduces the TCF/LEF activity, also reduces LV remodeling after MI injury (26). These conflicting data are probably due to the differences in target molecules and the downstream signaling. Although TT-10 has the weaker GSK3β inhibitory activity than BIO, the proliferative activity of TT-10 is much stronger than BIO. These results also suggest that the CM proliferative activity is attributed not only to the increasing transcriptional activity of β-catenin, but also to different signal transduction pathways and mechanisms. Recent studies have demonstrated the intimate relation between Wnt/β-catenin and Hippo signaling pathways. Wnt ligands can promote the YAP/TAZ-

FIGURE 6 TT-10 Enhances Proliferation of Existing CMs, and Decreases ROS and DNA Damage After MI

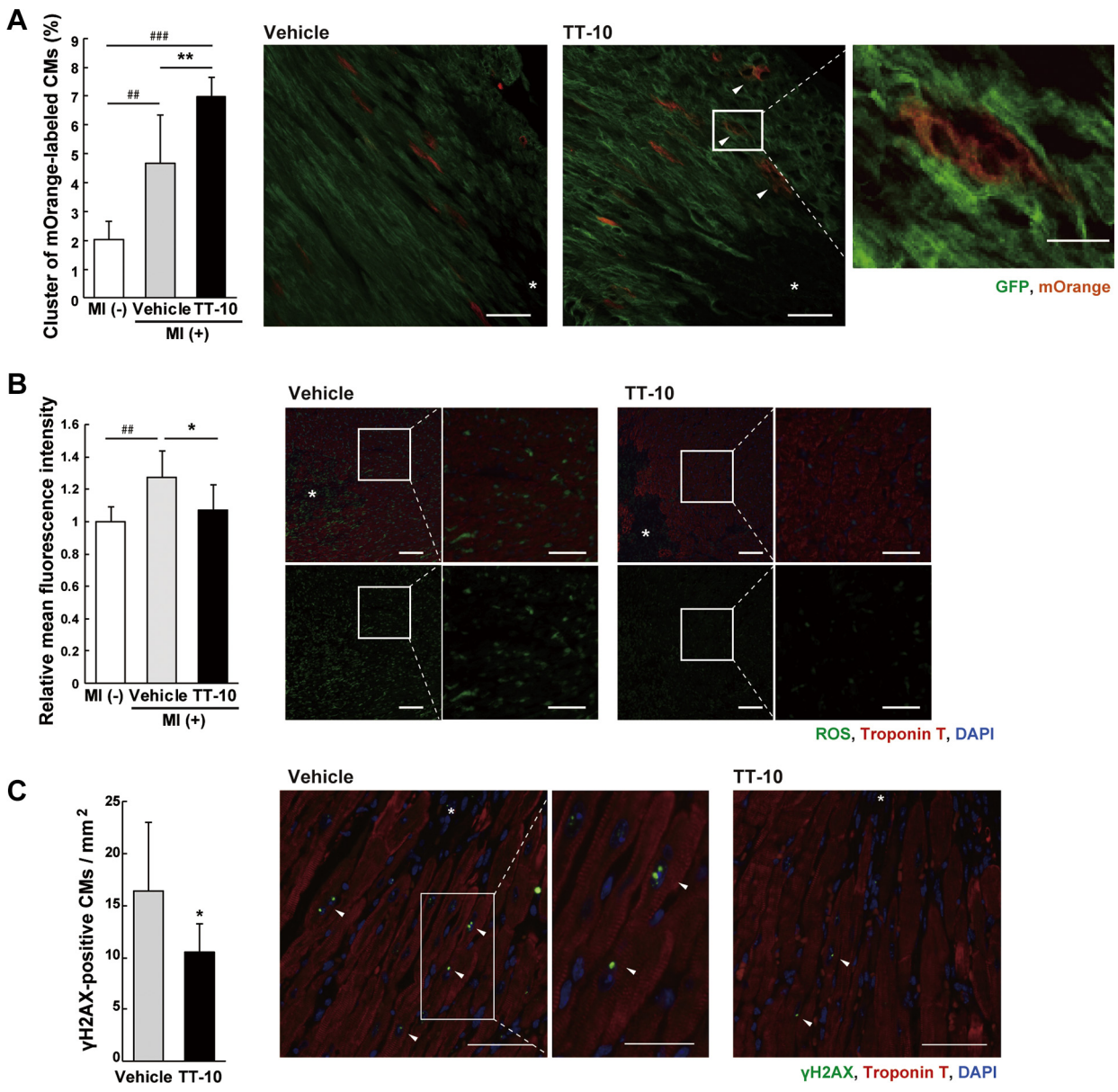

(A) The percentage of mOrange-labeled clustered CMs in α*MHC-MerCreMer*; *Rosa26*$^{rbw/+}$ mice. The increase from the background (MI [−]) indicates the proliferation of existing CMs (clonal expansion). Representative images of infarct border-zone myocardium are shown. Inset images were enlarged by confocal microscopy. **Arrowheads** indicate positive CMs; **white asterisk** indicates infarct area. n = 6 (MI [−]), 7 (vehicle), and 6 (TT-10). Scale bars: 100 μm; 25 μm in inset. **(B)** The relative mean fluorescence intensity for measuring ROS generation, detected by a mainly nuclear localized ROS-sensitive CellROX Green probe. Mean fluorescence intensity in the infarct border-zone myocardium relative to that in MI [−] mouse myocardium was shown. Representative images of infarct border-zone are shown. **White asterisk** indicates infarct area. n = 7 (MI [−]), 7 (vehicle), and 8 (TT-10). Scale bars: 100 μm; 50 μm in inset. **(C)** Quantitative analyses of γH2AX-positive CMs in the infarct border-zone 1 week after MI, with representative images. **Arrowheads** indicate positive CMs; **white asteris**k indicates infarct area. n = 10 (vehicle), and 12 (TT-10). Scale bars: 50 μm; 25 μm in inset. *p < 0.05, **p < 0.01 versus vehicle control. ##p < 0.01, ###p < 0.001 versus non-MI baseline. Abbreviations as in Figures 1, 4, and 5.

TEADs transcriptional activities in certain cell lines (27), and YAP interacts with β-catenin to transactivate *Snai2* and *Sox2* genes for cardiac growth in embryonic cardiac progenitor cells (7). Further studies are necessary to reveal the detailed relation between Wnt/β-catenin and Hippo signaling pathways after TT-10 treatment.

TT-10 activates the NRF2-mediated antioxidant responses in cultured CMs and reduces ROS production in vivo after MI, which might contribute to the promotion of exiting CMs proliferation, in addition to the reduction of cardiac fibrosis. Previous reports demonstrated that ROS-induced activation of the DNA damage response pathway is an important mediator of cell-cycle arrest and that increased ROS production in the heart after birth and/or injury reduces the CM proliferative activity (5). Because increased expression of NRF2 does not necessarily promote the DNA synthesis in cultured CMs (Supplemental Figure 8B) and neonatal hearts in *Nrf2* knockout mice cannot regenerate completely after MI (28), antioxidant mediators such as NRF2 may be necessary for promoting the CM proliferation and cardiac regeneration under hypoxic conditions but not sufficient.

Recently, fluorine-containing drugs, such as TT-10, have gained considerable attention because of the metabolic stability of the carbon-fluorine bond against enzymatic degradation, which is presumably useful to increase the in vivo bioavailability (17), and intraperitoneal TT-10 treatment after MI resulted in favorable cardiac outcomes. Therefore, TT-10 and/or the metabolites might also be pharmacologically active in vivo, although drug metabolism and pharmacokinetics studies must be performed to examine the absorption, distribution, metabolism, and excretion.

CONCLUSIONS

We developed a novel multifaceted fluorinated compound TT-10 with promising features of CM proliferative, antioxidant, and antiapoptotic activities in vitro. The intraperitoneal injection of TT-10 in mice after MI promoted CM proliferation and reduced infarct size and fibrosis, which resulted in amelioration of cardiac dysfunction. Stimulating endogenous CM proliferation and/or protection with TT-10 treatment may be a desirable strategy to complement current therapies for acute MI.

ACKNOWLEDGMENTS The authors thank Zeyu Yang, Kazutoshi Inami, and Fumiyoshi Michishita for the contributions to the initial screenings of YAP-TEAD activators; and thank Y. Ishiyama for excellent animal care and technical assistance.

ADDRESS FOR CORRESPONDENCE: Dr. Issei Komuro, Department of Cardiovascular Medicine, The University of Tokyo Hospital, 7-3-1 Hongo, Bunkyo-ku, Tokyo 113-8655, Japan. E-mail: komuro-tky@umin.ac.jp; OR: Dr. Masanobu Uchiyama, Graduate School of Pharmaceutical Sciences, The University of Tokyo, 7-3-1 Hongo, Bunkyo-ku, Tokyo 113-0033, Japan. E-mail: uchiyama@mol.f.u-tokyo.ac.jp; OR: Dr. Norifumi Takeda, Department of Cardiovascular Medicine, The University of Tokyo Hospital, 7-3-1 Hongo, Bunkyo-ku, Tokyo 113-8655, Japan. E-mail: notakeda-tky@umin.ac.jp.

PERSPECTIVES

COMPETENCY IN MEDICAL KNOWLEDGE: Many cell-based therapies for advanced heart failure are currently in progress, using bone marrow cells, mesenchymal stem cells, cardiac progenitor cells, and embryonic stem/iPS-derived CMs. Cellular injections might have temporally some beneficial effects, but most injected cells do not survive and engraft in the host myocardium, nor do they substantially transdifferentiate into new CMs. Rather, it is suggested that paracrine factors from transplanted cells and/or reactive immune cells stimulate division of existing CMs. The development of pharmacological strategies to stimulate this endogenous CM proliferation may provide a rational alternative treatment or complement current therapies for advanced heart failure.

TRANSLATIONAL OUTLOOK: A novel fluorine compound TT-10 ($C_{11}H_{10}FN_3OS_2$) was developed by targeting the pro-proliferative YAP and TEAD activities. TT-10 additionally exerts antioxidant and antiapoptotic activities, which would be beneficial for the survival of damaged CMs. Fluorine-containing molecules are expected to exhibit increased metabolic stability, and TT-10 treatment ameliorated experimental MI model in mice. Further in vivo studies in larger animal models are necessary to evaluate the drug metabolism, long-term safety, and effectiveness of TT-10 in acute MI.

REFERENCES

1. Bergmann O, Bhardwaj RD, Bernard S, et al. Evidence for cardiomyocyte renewal in humans. Science 2009;324:98–102.

2. Senyo SE, Steinhauser ML, Pizzimenti CL, et al. Mammalian heart renewal by pre-existing cardiomyocytes. Nature 2013;493:433–6.

3. Porrello ER, Mahmoud AI, Simpson E, et al. Transient regenerative potential of the neonatal mouse heart. Science 2011;331:1078–80.

4. Poss KD, Wilson LG, Keating MT. Heart regeneration in zebrafish. Science 2002;298:2188–90.

5. Puente BN, Kimura W, Muralidhar S a, et al. The oxygen-rich postnatal environment induces cardiomyocyte cell-cycle arrest through DNA damage response. Cell 2014;157:565–79.

6. Bersell K, Arab S, Haring B, Kühn B. Neuregulin1/ErbB4 signaling induces cardiomyocyte proliferation and repair of heart injury. Cell 2009;138:257–70.

7. Heallen T, Zhang M, Wang J, et al. Hippo pathway inhibits Wnt signaling to restrain cardiomyocyte proliferation and heart size. Science 2011;332:458–61.

8. Xin M, Kim Y, Sutherland LB, et al. Hippo pathway effector Yap promotes cardiac regeneration. Proc Natl Acad Sci U S A 2013;110:13839–44.

9. Kodaka M, Hata Y. The mammalian Hippo pathway: regulation and function of YAP1 and TAZ. Cell Mol Life Sci 2015;72:285–306.

10. Naito AT, Shiojima I, Akazawa H, et al. Developmental stage-specific biphasic roles of Wnt/beta-catenin signaling in cardiomyogenesis and hematopoiesis. Proc Natl Acad Sci U S A 2006;103:19812–7.

11. Maruyama J, Inami K, Michishita F, et al. Novel YAP1 activator, identified by transcription-based functional screen, limits multiple myeloma growth. Mol Cancer Res 2018;16:197–211.

12. Yang Z, Nakagawa K, Sarkar A, et al. Screening with a novel cell-based assay for TAZ activators identifies a compound that enhances myogenesis in C2C12 cells and facilitates muscle repair in a muscle injury model. Mol Cell Biol 2014;34:1607–21.

13. Sohal DS, Nghiem M, Crackower MA, et al. Temporally regulated and tissue-specific gene manipulations in the adult and embryonic heart using a tamoxifen-inducible Cre protein. Circ Res 2001;89:20–5.

14. Rinkevich Y, Lindau P, Ueno H, Longaker MT, Weissman IL. Germ-layer and lineage-restricted stem/progenitors regenerate the mouse digit tip. Nature 2011;476:409–13.

15. Toko H, Takahashi H, Kayama Y, et al. ATF6 is important under both pathological and physiological states in the heart. J Mol Cell Cardiol 2010;49:113–20.

16. Eulalio A, Mano M, Dal Ferro M, et al. Functional screening identifies miRNAs inducing cardiac regeneration. Nature 2012;492:376–81.

17. Müller K, Faeh C, Diederich F. Fluorine in pharmaceuticals: looking beyond intuition. Science 2007;317:1881–6.

18. Sakaue-Sawano A, Kurokawa H, Morimura T, et al. Visualizing spatiotemporal dynamics of multicellular cell-cycle progression. Cell 2008;132:487–98.

19. Hahn JY, Cho HJ, Bae JW, et al. β-catenin overexpression reduces myocardial infarct size through differential effects on cardiomyocytes and cardiac fibroblasts. J Biol Chem 2006;281:30979–89.

20. Naito AT, Shiojima I, Komuro I. Wnt signaling and aging-related heart disorders. Circ Res 2010;107:1295–303.

21. Tseng AS, Engel FB, Keating MT. The GSK-3 inhibitor BIO promotes proliferation in mammalian cardiomyocytes. Chem Biol 2006;13:957–63.

22. Taguchi K, Motohashi H, Yamamoto M. Molecular mechanisms of the Keap1-Nrf2 pathway in stress response and cancer evolution. Genes to Cells 2011;16:123–40.

23. Chen Z, Siu B, Ho YS, et al. Overexpression of MnSOD protects against myocardial ischemia/reperfusion injury in transgenic mice. J Mol Cell Cardiol 1998;30:2281–9.

24. Hara H, Takeda N, Komuro I. Pathophysiology and therapeutic potential of cardiac fibrosis. Inflamm Regen 2017;37:13.

25. Kim YS, Jeong H, Kim AR, et al. Natural product derivative BIO promotes recovery after myocardial infarction via unique modulation of the cardiac microenvironment. Sci Rep 2016;6:30726.

26. Laeremans H, Hackeng TM, Van Zandvoort MAMJ, et al. Blocking of frizzled signaling with a homologous peptide fragment of Wnt3a/Wnt5a reduces infarct expansion and prevents the development of heart failure after myocardial infarction. Circulation 2011;124:1626–35.

27. Azzolin L, Panciera T, Soligo S, et al. YAP/TAZ incorporation in the β-catenin destruction complex orchestrates the Wnt response. Cell 2014;158:157–70.

28. Tao G, Kahr PC, Morikawa Y, et al. Pitx2 promotes heart repair by activating the antioxidant response after cardiac injury. Nature 2016;534:119–23.

KEY WORDS antioxidation, Hippo pathway, myocardial infarction, regeneration, Wnt/β-catenin signaling

APPENDIX For an expanded Methods section and supplemental figures, please see the online version of this paper.